Available online at www.sciencedirect.com
SCIENCE DIRECT
Polymer 47 (2006) 6057–6065
polymer
www.elsevier.com/locate/polymer

The effect of functionalized nanoparticles on thiol–ene polymerization kinetics

Tai Yeon Lee [a], Christopher N. Bowman [a,b,*]

[a] Department of Chemical and Biological Engineering, University of Colorado at Boulder, Boulder, CO 80309, USA
[b] Dental School, University of Colorado Health Science Center, Denver, CO 80045-0508, USA

Received 8 February 2006; received in revised form 2 June 2006; accepted 6 June 2006
Available online 10 July 2006

Abstract

Functionalized silica nanoparticles with thiol or acrylate groups were synthesized, and the effect of the functionalized particles on the thiol–ene photopolymerization kinetics was investigated by real-time FTIR spectroscopy. To explain the effect of the nanoparticles on thiol–ene polymerization kinetics, the thiol–ene polymerization at the interface of the particle and the bulk monomer was studied in conjunction with the effects of light intensity and viscosity changes caused by the nanoparticles. These results are compared with corresponding nanofilled acrylate systems. Nanoparticles were not found to significantly affect the polymerization of acrylate-based nanocomposites regardless of the functional group type attached to the particle surface while significant changes in polymerization kinetics were observed with thiol–ene based nanocomposites. The thiol–ene polymerization rate decreases with increasing particle content for small amounts of particle loadings due to a stoichiometric imbalance of thiol and ene groups at the particle surface. However, the polymerization rates increase with larger particle loadings because of polymerization viscosity enhancements. Thiol–ene based nanocomposites exhibit higher final conversions than acrylate systems, reduce the oxygen inhibition relative to acrylate polymerizations, and still react rapidly to form highly crosslinked, hard, high glass transition temperature materials.

Keywords: Thiol–ene; Nanocomposites; Polymerization kinetics

1. Introduction

A great deal of interest has recently focused on hybrid organic–inorganic photopolymerization reactions [1–10] as photopolymerization provides a simple method for *in situ* production of nanocomposite films from inorganic particle-dispersed organic monomer formulations. Conventional hybrid composite formation processes such as melt mixing of linear polymers with fillers and solvent based processes have many problems including the release of volatile organic compounds, thermal degradation of the polymer, multi-step processing, and high cost. On the other hand, photopolymerization eliminates these problems and has many advantageous aspects with respect to enhanced performance of the resultant products and utilization of simple and efficient processing techniques [11,12]. In photocured materials, enhanced properties such as hardness, strength, and chemical resistance are obtained. Also, spatial and temporal control of curing, short curing times, and solvent free processing are all possible for photocurable polymeric nanocomposites. In conjunction with these advantages of photopolymerizations, incorporating inorganic nanoparticles into photocurable monomers is a desirable method for generating high performance materials. Dispersion of nanosize inorganic particles in a polymer matrix results in molecular level mixing between the polymeric chains and the particles. Furthermore, covalent interfacial coupling of

* Corresponding author. Department of Chemical and Biological Engineering and Restorative Dentistry, University of Colorado and University of Colorado Health Sciences Center, ECCH 111 Campus Box 424, Boulder, CO 80309-0424, USA. Tel.: +1 303 492 3247; fax: +1 303 492 4341.
E-mail address: bowmanc@buffmail.colorado.edu (C.N. Bowman).

0032-3861/$ - see front matter © 2006 Elsevier Ltd. All rights reserved.
doi:10.1016/j.polymer.2006.06.034

nanoparticles with the polymer matrix via modification of the particle surface with polymerizable reactive groups reinforces polymeric materials and improves properties such as hardness, scratch resistance, thermal conductivity, and polymerization shrinkage without sacrificing optical properties [1–3]. In particular, polymeric nanocomposites are attractive in surface coatings because surface and bulk properties are tailored by modifying the surface functionality of the nanoparticles.

An emerging area in photopolymerizations relates to thiol–ene polymerizations. Thiol–ene polymerizations have an extensive list of advantages in regards to the polymerization processes and resulting polymer properties. These reactions are free-radical reactions that proceed by a step-growth mechanism involving a free-radical addition followed by a chain-transfer reaction [13–17]. In thiol–ene polymerizations a broad spectrum of physical properties is achieved because a wide variety of enes such as acrylate, vinylether, allyl ether, vinyl acetate, and alkene are used. Also, flexibility, high refractive index, and reduced swelling are all obtained from thiol–ene polymers [14,15]. In conjunction with these advantages, delayed gelation [18], low polymerization shrinkage [14,19], reduced oxygen inhibition [14,15,20], photoinitiatorless polymerization [20–22], and homogeneous polymer structures of thiol–ene polymerizations promise thiol–ene polymers as high performance materials. However, further improvements of surface and bulk properties of thiol–ene coatings are highly desirable because hard thiol–ene coatings are not easily attainable due to limited availability of rigid monomer structures, low crosslink density compared to (meth)acrylates, and flexible thioether linkages.

Therefore, the development of inorganic nanoparticle/thiol–ene nanocomposites should be one of the most interesting areas in photopolymerization research. For this research, it is important to understand the effect of nanoparticles on the thiol–ene photopolymerization kinetics. Fundamental understanding of the polymerization kinetics provides information to design the polymer network structures and properties of nanocomposites. Previous research has reported on (meth)-acrylate-based photocurable nanocomposites and the effect of nanoparticles on polymerization has not been clearly investigated. It was reported that the polymerization rates of (meth)acrylate-based nanocomposites increased or decreased based on the filler types and the monomers used [2–6, 8–10]. Several explanations for increased or decreased polymerization rates such as termination kinetics, viscosity effects, and light scattering effects have been suggested, but little evidence has been provided [4–6].

In thiol–ene polymerizations because of the step-growth mechanism of thiol and ene monomers, a stoichiometric balance of the two functional groups is critical to obtain high conversion and appropriate polymeric networks. In thiol–ene reaction, prior to achieving high conversion, the polymerization medium viscosity is lower and is relatively less important as compared to chain polymerizations of (meth)acrylates which form highly crosslinked microgels at the very initial stages of polymerization [14,15]. Therefore, the polymerization kinetics of thiol–ene nanocomposites could be significantly different from (meth)acrylate-based nanocomposites. Herein, we describe the effect of thiol functionalized nanoparticles on thiol–ene photopolymerization kinetics. The polymerization at the particle surface where thiol–ene monomers and particle surface thiol groups exist is discussed. Light intensity and viscosity changes caused by the particles are also investigated to explain the polymerization kinetics of thiol–ene nanocomposites. Also, acrylate nanocomposite systems are studied as a control system and used to compare with the corresponding thiol–ene systems.

2. Experimental

2.1. Materials

1,3,5-Triallyl-1,3,5-triazine-2,4,6(1*H*,3*H*,5*H*)-trione (TATATO), 1,6-hexanedithiol (HDT), anhydrous toluene, triethylamine, tetrahydrofuran, ethanol, methylene chloride, and diethylamine were obtained from Aldrich. 3-Acryloxypropyl trichlorosilane was purchased from Gelest Inc. The photoinitiator, 2-hydroxy-2-methyl-1-phenyl propan-1-one (D1173), was purchased from Ciba-Geigy. 1,6-Hexanediol diacrylate and silica nanoparticles (OX-50, primary particle size 40 nm) were donated by Cytec (Smyrna, GA) and Degussa, respectively. 16 Functional thiol (Boltorn H20-3MP) was donated by Bruno Bock. All monomers and the photoinitiator were used as received.

2.2. Immobilization of the chlorosilanes on silica nanoparticle

The silica nanoparticles (40 nm, 1.0 g) were dried at 150 °C for 3 h under high vacuum to remove moisture and then were dispersed in dry toluene (50 ml) by vigorous agitation and ultrasonication for 30 min. Trichlorosilane (1.0 g) in a solution of dry toluene (10 ml) was added dropwise followed by triethylamine (1 ml). The reaction mixture was stirred under nitrogen for 18 h. After the reaction, the particles were washed seven times with toluene, ethanol, ethanol/water mixture (2×), ethanol, and THF (2×). After washing with each solvent, the particles were isolated by centrifugation. The functionalized particles were then dried in a vacuum oven at room temperature for 24 h and obtained as a white powder.

2.3. Immobilization of thiols to SAM surfaces on silica nanoparticle

Silica nanoparticles modified with acrylate groups (1.0 g) were added in CH_2Cl_2 (50 ml). The particles were dispersed by vigorous agitation (30 min) and sonication (30 min) to reduce aggregation. 16 Functional thiol (4 g) was added and then the reaction mixtures were agitated for 30 min. Catalytic amounts of diethylamine (10 drops) were added and stirred at room temperature for 24 h. The resultant particles were washed with $MeCl_2$ (5×) and centrifuged at 3000 rpm for 10 min.

2.4. Methods

The kinetic profiles of the UV-induced polymerizations were studied using real-time FTIR, a Nicolet 750 Magna FTIR spectrometer with a KBr beam splitter and an MCT detector. Infrared spectra were recorded on a spectrometer designed to allow light to impinge on a horizontal sample using a fiber-optic cable. A modified horizontal transmission unit was designed to prevent sample flow. The real-time FTIR setup has been illustrated elsewhere [23]. Monomer samples with thicknesses of about 25 μm were placed between two sodium chloride plates while the FTIR sample chamber was continuously purged with dry air. The series of infrared absorption spectra was obtained under continuous UV irradiation with 3.5 scans/s. The concentration of ene double bonds during polymerization was monitored at 3080 cm^{-1} and 1636 cm^{-1} while the thiol functional group was monitored at 2575 cm^{-1}. Conversions were calculated using the ratio of peak areas as a function of time to the peak area prior to polymerization. All reactions were performed under ambient conditions. Polymerizations were initiated via an EXFO Acticure light source (EXFO, Mississauga, Ontario) with a 320–500 nm filter. Irradiation intensities were measured with an International Light, Inc., model IL1400A radiometer (Newburyport, MA).

The viscosity of the inorganic particle/thiol–ene monomer mixtures was measured using a Brookfield CAP 2000+ Viscometer (Cone & Plate Type) at 25 °C.

UV Light attenuation by nanocomposite films was measured using the radiometer. After curing 30 μm thick films, the films were placed on the top of the radiometer sensor. Initial light intensity was set to 10 mW/cm^2. The changes of light intensity with and without polymer films were recorded five times for each sample, and average values were used.

3. Results and discussions

Generally, unmodified silica particles having hydroxyl surface functional groups cause severe particle aggregation due to strong hydrogen bonding interactions between the particles coupled with poor compatibility of the particles with the monomer mixtures. This behavior often results in deleterious effects on the cured nanocomposites such as poor particle dispersion and reduced mechanical properties. Functional groups on the particle surface which can participate in the polymerization provide covalent interactions between the particles and the polymer resins. These interactions strengthen the particle surface–resin interface, resulting in enhanced mechanical properties [1,2]. In this study, we modified the particle surface with thiol functional groups to be used as a polymerizable component in the thiol–ene polymerization. To do so, acrylate groups were first attached to the particles by sequential hydrolysis and condensation reactions of acryloxypropyl trichlorosilane and then thiol groups were introduced by an amine-catalyzed Michael addition reaction [24,25] between multifunctional thiols and surface acrylate groups. Fig. 1 shows the FTIR spectra of silica nanoparticles before and after the modification with an acrylate and a thiol functional group. Unmodified

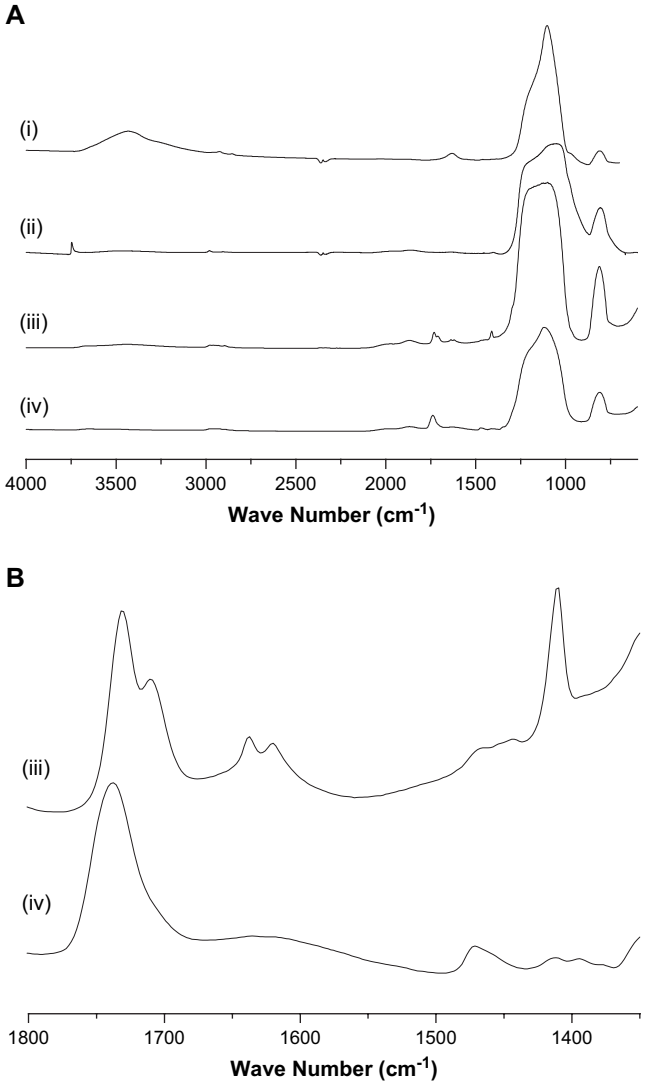

Fig. 1. (A) IR spectra of (i) unmodified before drying, (ii) unmodified after drying, (iii) acrylated, and (iv) thiolated silica nanoparticles. (B) IR spectra of (iii) acrylated and (iv) thiolated silica nanoparticles in 1800–1300 cm^{-1} region.

particles show a silicon ether peak around 1100 cm^{-1} and a broad hydrogen bonded hydroxyl peak around 3500 cm^{-1}. After drying, the hydrogen bonded hydroxyl peak disappears and a sharp free hydroxyl peak is observed at 3750 cm^{-1}. The particles functionalized with a 3-acrylolpropyltrichlorosilane show acrylate peaks at 1630 cm^{-1} (C=C stretching) and at 1406 cm^{-1} (C=C–H bending). The IR spectrum of the thiol functionalized particles shows no residual acrylate groups, indicating that the multifunctional thiol groups react with the acrylate double bonds, and the particle surface is highly functionalized with thiol groups. The thiol peak at 2575 cm^{-1} is not observed due to the low molar absorption coefficient of the thiol groups.

After the modification of the particle surface with specific functional groups, the most popular method to measure the concentration of the functional groups attached to the particle surface is a thermogravimetric method [26] which measures very small changes in weight loss during a heating process.

Here, one advantageous aspect of an amine-catalyzed Michael addition reaction should be noted. An amine-catalyzed Michael addition reaction is a stoichiometric reaction between an electron poor double bond such as an acrylate and a thiol [24,25]. Therefore, here, the amount of acrylate groups attached to the particles is calculated by measuring the amount of thiols reacting with acrylate double bonds during this reaction. Fig. 2 shows the IR spectra before and after an amine-catalyzed Michael addition reaction between the acrylated particles and hexanedithiol (HDT). The peak intensity of the acrylate double bond at 1406 cm^{-1} decreased 75% and the thiol peak area at 2575 cm^{-1} reduced 10%. Based on the conversion of both functional groups and the concentration of the acrylated particles and thiols used, it was calculated that 4.5×10^{-4} mol of acrylate double bonds are present in 1 g of particles. The thiol concentration in thiol functionalized particles was not measurable due to its low molar absorption coefficient. However, it is expected that the thiol concentration should be at least as high as that of the acrylate group because a multifunctional thiol was used for the modification.

When polymerizable functional groups are attached to particles, they affect the polymerization kinetics of nanocomposites because of the different geometric environment for polymerization at the particle surface and/or the particle–monomer interface. Fig. 3 shows the effect of thiol functionalized nanoparticles on the polymerization kinetics of triallyl triazine trione (TATATO)/1,6-hexanedithiol (HDT) 1:1 molar mixtures. The polymerization rate and final conversion of the nanocomposites do not show significant changes as shown in Fig. 3(a). However, an interesting tendency is observed with increasing particle content for small loading levels (Fig. 3(b)). Up to 5 wt% of the thiol functionalized particles, polymerization rates decrease; however, the rate increases with further loading of the particles from 5 to 33 wt% particles. Based on these results, the polymerization kinetics of the thiol–ene nanocomposites are affected by more than two factors which

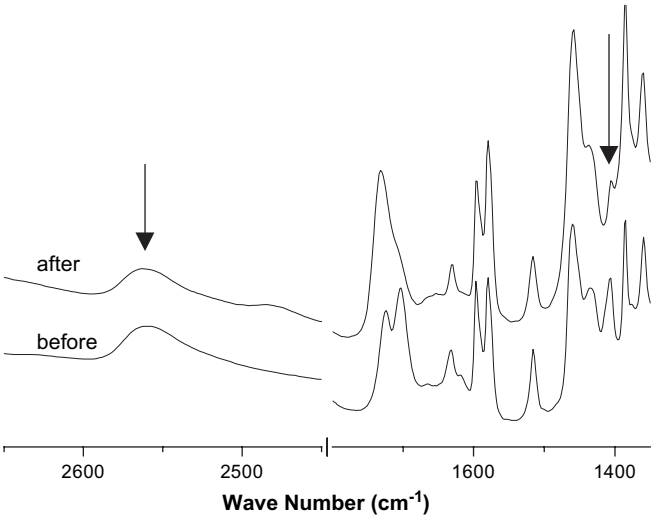

Fig. 2. IR spectra before and after an amine-catalyzed Michael addition reaction between acrylated particles and hexane dithiol. Hexanedithiol (3.176×10^{-4} mol), 0.1 g of acrylated particles, and 1 ml of $MeCl_2$ as a solvent were used.

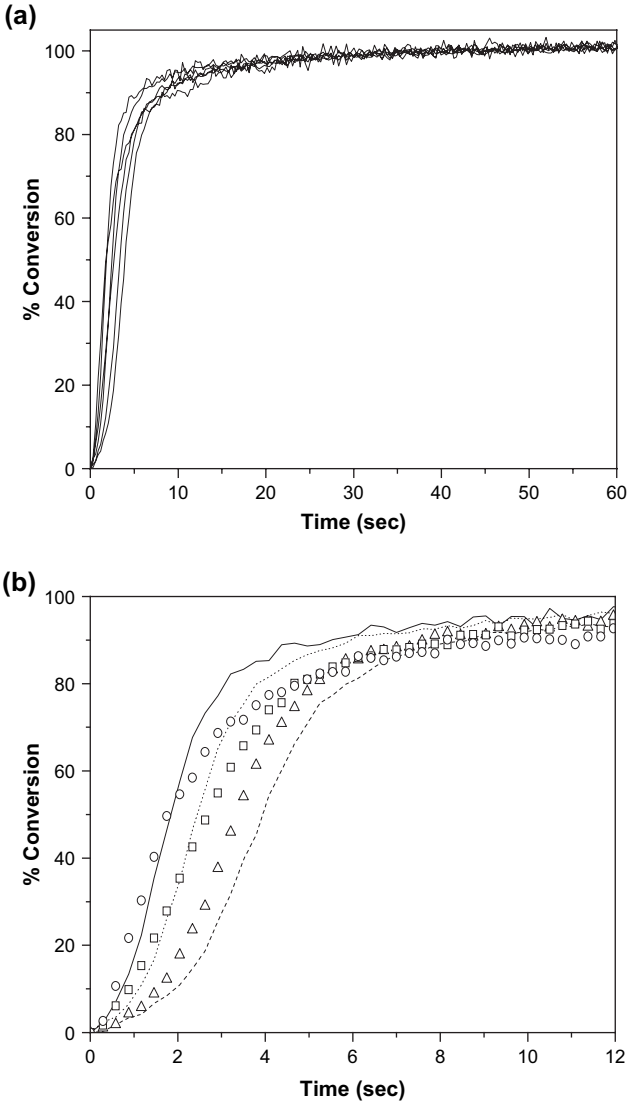

Fig. 3. The functional group conversion versus time plots of triallyl triazine trione (TATATO)/1,6-hexanedithiol (HDT) 1:1 molar mixtures as a function of thiolated particle content; 0 wt% (solid line), 1 wt% (dot), 5 wt% (dash), 10 wt% (△), 23 wt% (□), and 33 wt% (○). Profiles are shown for the initial (a) 60 s and (b) 12 s. Samples contain 0.5 wt% D1173 and are irradiated at 14.5 mW/cm^2 using 320–500 nm light.

enhance or suppress the polymerization rates. Light scattering by the particles, the nature of the polymerizations at the monomer–particle interface, and the mixture viscosity are all possible explanations for the results.

First, to investigate the effects of surface functional groups on thiol–ene polymerizations, the polymerization kinetics of the thiol–ene nanocomposites with unmodified particles were examined. Fig. 4 shows the conversion versus time plots of TATATO/HDT 1:1 molar mixtures containing different amounts of unmodified nanoparticles which have silanol groups on the surface. Interestingly, the polymerization rates are independent of the particle content added. For the entire range of irradiation time, the polymerization rate and final conversion are identical for all samples. The only difference between the particles used in Figs. 3 and 4 is the presence of polymerizable thiol groups on the thiol functionalized particles. This result

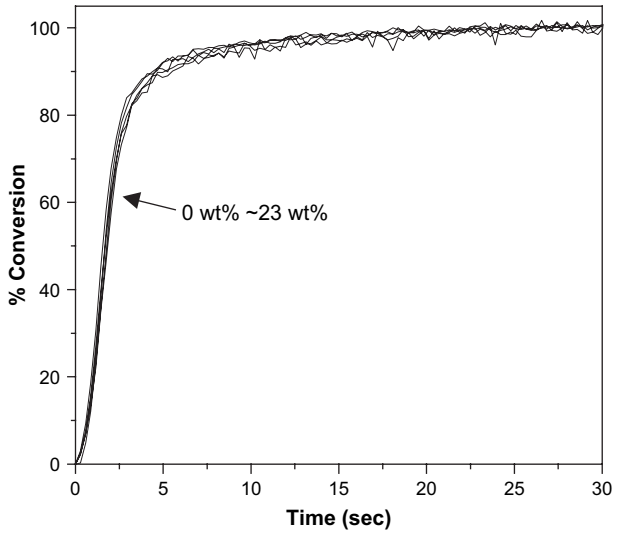

Fig. 4. The functional group conversion as a function of time for TATATO/HDT 1:1 molar mixtures as a function of unmodified particle content (0–23 wt%). Samples contain 0.5 wt% D1173 and are irradiated at 4.5 mW/cm^2 using 320–500 nm light.

strongly indicates that thiol functional groups on the particle surface are participating in the polymerization reaction and affecting the thiol–ene polymerization kinetics.

To explain the effect of thiol functional groups on polymerization kinetics, the polymerizations at the interface between the thiolated nanoparticles and bulk monomer should be considered. A diagram illustrating the chemical composition at the particle–monomer interface is suggested in Fig. 5(a). Because of the high thiol group concentration at the particle surface, it is expected that there is a stoichiometric imbalance between thiol and ene groups (large excess of thiol) at the particle surface. Also, the mobility of the thiyl radicals on the surface should be lower than those in the bulk. Because a stoichiometric imbalance between the thiol and ene groups is critical in thiol–ene polymerization kinetics, thiol–ene polymerization kinetics at the particle–monomer interface should be different from those in the bulk monomer phase (Fig. 5(b)). This indicates that there are two different polymerization environments in the nanocomposite systems studied, and the reaction scheme for both is described below.

As mentioned previously, thiol–ene polymerizations proceed by a two step mechanism including both chain transfer and propagation [14,15]. The chain-transfer reaction rate constant (k_{CT}) and the propagation rate constant (k_p) should be similar for both circumstances. However, the overall chain-transfer reaction rate is faster at the particle surface than in the bulk due to the presence of excess thiols on the surface. The propagation rate is slower at the interface than in the bulk because of a lower ene concentration and hindered mobility of the surface thiyl radicals. Also, due to the low ene concentration at the particle surface, the thiyl radicals have a much higher probability of undergoing a chain-transfer reaction to other surface thiols and a termination by recombination of two thiyl radicals. This local functional group imbalance at the surface reduces the overall polymerization rates of the

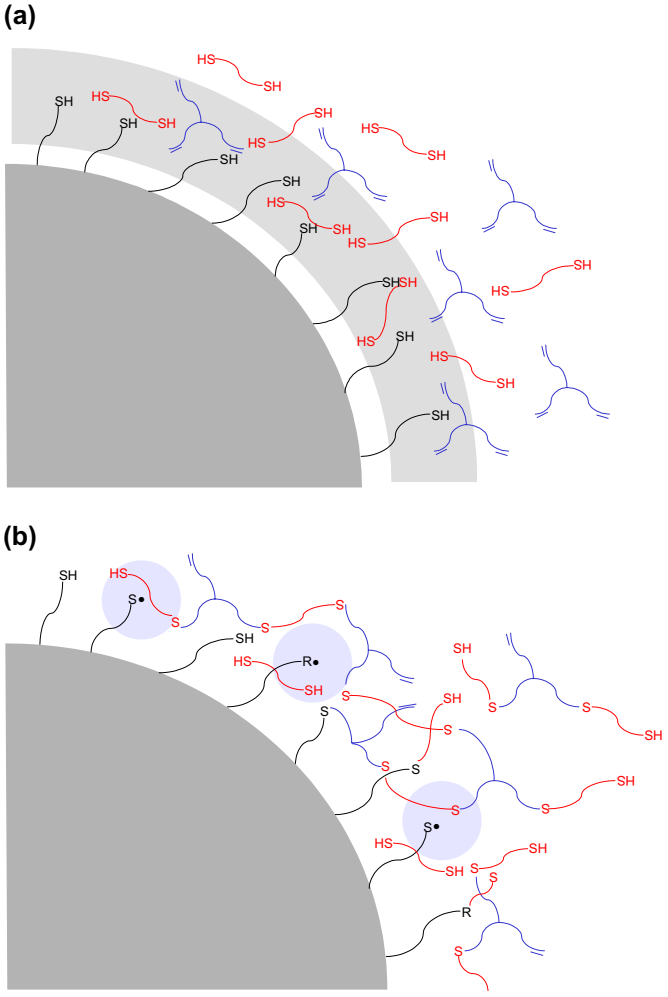

Fig. 5. A diagram illustrating the chemical composition at the particle surface of a thiolated nanoparticle/thiol–ene mixture (a) before and (b) during polymerization.

thiol–ene polymerization. As particle content is increased, particle–monomer interface volume where excess thiol groups exist increases and the polymerization rate decreases.

$$
\begin{array}{lllll}
 & = & + \ SH_1\,(Bulk) & + & SH_2\,(surface) \\
\text{chain transfer} & R\bullet + SH_1 \xrightarrow{k_{CT}} & S_1\bullet & (bulk) & \\
 & R\bullet + SH_2 \xrightarrow{k_{CT}} & S_2\bullet & (surface) & \\
\text{propagation} & S_1\bullet + = \xrightarrow{k'} & R\bullet & (bulk) & \\
 & S_2\bullet + = \xrightarrow{k''} & R\bullet & (surface) &
\end{array}
$$

To provide further evidence of reduced polymerization rates due to stoichiometric imbalance, three model systems were investigated and the results are shown in Fig. 6. First is the result for an acrylated particles/hexanediol diacrylate (HDDA) nanocomposite system. In this case, the acrylate represents the only polymerizable functional group both in particles and monomers so there is no concentration imbalance of polymerizable functional groups at the particle–monomer interface. If the stoichiometric imbalance is the primary reason

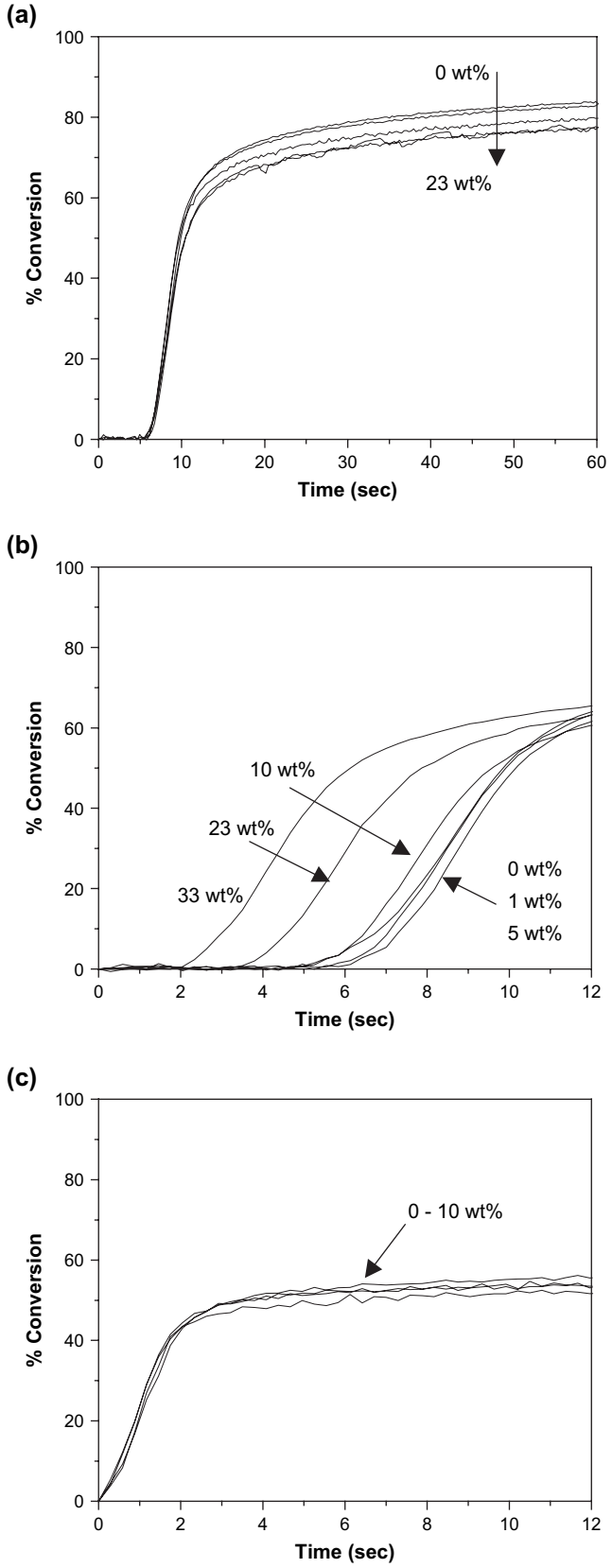

Fig. 6. The functional group conversion versus time for (a) HDDA/acrylated particles, (b) HDDA/thiolated particles, and (c) TATATO/HDT/thiolated particles with a 1:2 molar mixture of thiol:ene maintained as a function of particle content (0–23 wt%). Samples contain 0.5 wt% D1173 and are irradiated at 4.5 mW/cm^2 using 320–500 nm light.

for the reduced polymerization, it is expected that acrylated particles should have no effect on the polymerization of HDDA. Fig. 6(a) shows the conversion versus time plots of acrylated particle/HDDA mixtures. The mixtures of acrylated particles/HDDA show no change in polymerization rates regardless of the particle amounts incorporated. Because of dissolved oxygen in the HDDA, all samples show an induction period prior to polymerizations. Secondly, the effect of thiol functionalized particles on HDDA polymerization was investigated and is shown in Fig. 6(b). The polymerization of HDDA containing thiol functionalized particles yields a somewhat different result. With increasing thiol functionalized particle content, it is clearly shown that the induction period decreases significantly. The thiol functional groups on the particles react with peroxy radicals resulting in a reduced induction period. This reduction indicates that the particle surface is indeed functionalized with thiol groups which are not observed in the IR spectrum due to the low molar absorption coefficient (Fig. 1). However, once started, the polymerization rates are almost identical as expected from the slopes of the conversion curves of each sample. Actually, the thiol groups can decrease the HDDA polymerization rate when the thiol concentration is high. However, it is reported that in acrylate/thiol mixtures, acrylate functional groups undergo much faster polymerization than thiol functional groups [28,29] and small amounts of thiols do not appreciably change the acrylate polymerization kinetics in nitrogen [30]. Finally, another interesting result supporting reduced thiol–ene polymerization rates by stoichiometric imbalance is shown in Fig. 6(c): conversion versus time plots of 1:2 thiol:ene mixtures with different amounts of thiol functionalized particles. As shown in Fig. 6(c), final ene conversions reach approximately 50% due to the 1:2 thiol:ene molar ratio. The conversion rates of the samples do not show any change as a function of particle content. These results indicate that in 1:2 thiol:ene mixtures, the ene concentration at the particle surface is closer to the thiol concentration at that interface. Therefore, there is a reduced stoichiometric imbalance between the thiol and ene functional groups, resulting in almost identical polymerization rates.

The polymerization rate changes of inorganic particle/organic nanocomposites also happen when UV light is scattered or reflected by particles. However, the nanoscale size of the particles, good dispersion, and the relatively thin sample lead to relatively uniform light exposure throughout the sample thickness. The monomer/nanoparticle mixtures used in this study are transparent with only a slight opacity. Fig. 7 shows the reduction of light intensity by thiol–ene and HDDA based cured nanocomposite films with thicknesses of approximately 30 μm. The light intensity decrease is more pronounced with increasing nanoparticle content. However, the extent of reduction in light intensity is quite small even with 23 wt% nanoparticles. Thiol–ene and HDDA composites with 23 wt% particles show about 17% and 6% reduction in light intensity, respectively. It is expected that the additional reduction of light intensity in the thiol–ene sample might result from the high refractive index of thiol–ene mixtures relative to the acrylates.

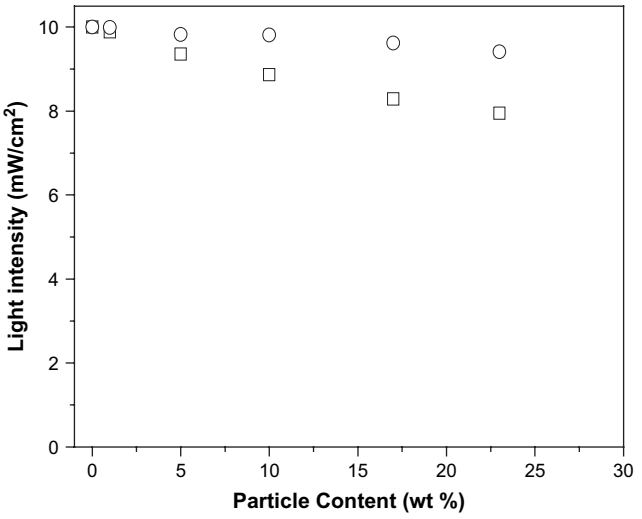

Fig. 7. The light intensity reduction by cured nanocomposite films; thiol–ene (□) and HDDA (○) based polymer composite films containing different amounts of thiol functionalized nanoparticles. Film thickness is 30 μm.

By measuring the intensity dependence of polymerization rates of thiol functionalized particle/thiol–ene mixtures, decreases in polymerization rates associated with scattered or reflected UV light can be calculated. For a neat thiol–ene mixture without particles, the polymerization rate is proportional to the light intensity to the 0.53 power which is consistent with the previous reports [27]. Also, thiol–ene mixtures containing 1–23 wt% of thiol functionalized particles showed almost the same dependence on light intensity (ranging from 0.52 to 0.54, standard deviation ± 0.0089). Based on this result, the termination reactions of thiol–ene polymerizations occur by a bimolecular reaction. This behavior indicates that the polymerization rate is proportional to the initiation rate to the 0.5 power which is proportional to the light intensity (i.e., $R_p \propto I^{0.5}$). For HDDA, the polymerization rate is proportional to ~0.7 power of the initiation rate ($R_p \propto I^{0.7}$) [31]. Based on the termination kinetics and the light intensity decrease measured, the polymerization rate on the bottom side of the sample in thiol–ene and HDDA composites containing 23 wt% of particles should be 10% and 3% slower than neat samples without particles, respectively. These explanations are consistent with Figs. 4 and 6 and indicate that light scattering and reflection by particles do not significantly affect polymerization rates.

Based on the above results, it is expected that the increased polymerization rates of thiol–ene nanocomposites are observed when large amounts of thiol functionalized particles are added resulting from different factors. One possible factor enhancing the polymerization kinetics of nanocomposite systems is the monomer mixture viscosity. Increased viscosity slows the termination kinetics due to reduced mobility of the growing polymer chains, which results in enhanced polymerization rates. For this reason, the viscosity of the thiol–ene nanocomposites was measured before polymerization. It was observed that the viscosity of the thiol–ene nanocomposites increased with increasing particle content as expected. The viscosity of the thiol–ene mixtures with 23 wt% of thiol functionalized particles (*218 mPa s*) has about 30 times higher viscosity than the neat thiol–ene mixture (*6.5 mPa s*). Therefore, we might expect that, as the particle content is increased, the higher viscosity results in enhanced polymerization rates. However, it should be noted that if we think about the viscosity of monomers and polymers at the molecular level, the viscosity increase in the nanocomposite should be considered differently from purely organic systems. If organic viscosity-modifiers are added to monomers, modifiers interact with monomers and growing polymer molecules so that the viscosity increases at the molecular level. However, in inorganic particle/monomer mixtures, the viscosity increases due to the presence of solid particles through interaction between particles and monomers at the particle interface. Thus, overall viscosity at the macroscale increases while the viscosity of the bulk monomer at the molecular level should remain nearly the same. Therefore, the effect of increased viscosity on polymerization should not be significant in nanocomposite systems. Also, in traditional thiol–ene systems, viscosity is not as important of a factor on polymerization kinetics. As mentioned earlier, thiol–ene monomers do not build up high molecular weight polymers and crosslinked gels at low conversion. This explanation is consistent with the previous results shown in Fig. 4. When unmodified particles are used, the polymerization rates of the unmodified particle/thiol–ene mixture do not change while the overall viscosity of the samples increases dramatically.

However, as the particle content increases so that the distance between particles in the monomer solution decreases significantly, the viscosity can lead to enhanced polymerization rates when polymerizable (thiol functionalized) particles are used. To explain this behavior, a diagram illustrating the crosslinked structure of a thiol–ene nanocomposite is presented in Fig. 8. In nanocomposites containing high particle content, only a few propagation steps are required to chemically connect each particle due to the proximity of particles as shown in Fig. 8(b). This proximity and coupling result in incorporation of particles into the crosslinked network at the initial stages of polymerization and lead to a huge increase in viscosity. This type of reaction-induced viscosity enhancement results in enhanced polymerization rates, especially at the initial stage. Fig. 9 shows normalized maximum R_p and relative average R_p versus particle content. Relative average R_p values were obtained by calculating $1/(t_0 - t_{50})$ and $1/(t_0 - t_5)$ values where t_0, t_5, and t_{50} are the times required to reach 0, 5, and 50% conversions, respectively. It is obvious that the maximum polymerization rates decrease up to 23 wt% particle loading then increase while relative average R_p is reduced up to 5 wt% particle content and then increases dramatically. These results indicate that initial polymerization rates are enhanced more than the maximum polymerization rates by particle addition. The sample containing 33 wt% particles (near the maximum loading) shows a significant increase in the initial average R_p value ($1/(t_0 - t_5)$). We observed that the polymerization rates of the sample containing 33 wt% particles are higher than the neat sample in Fig. 3(b), and this result strongly indicates acceleration due to the viscosity increase.

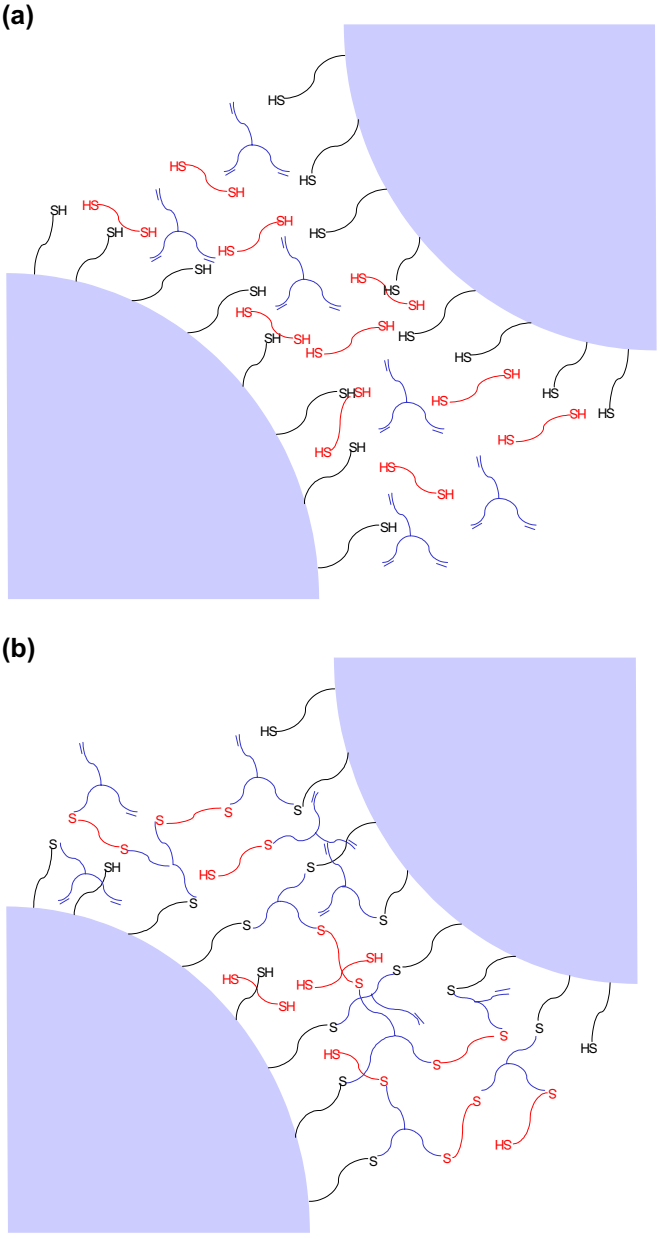

Fig. 8. A diagram illustrating the crosslinked structure of a thiol–ene nanocomposites with high contents of thiol functionalized particles (a) before and (b) during polymerization.

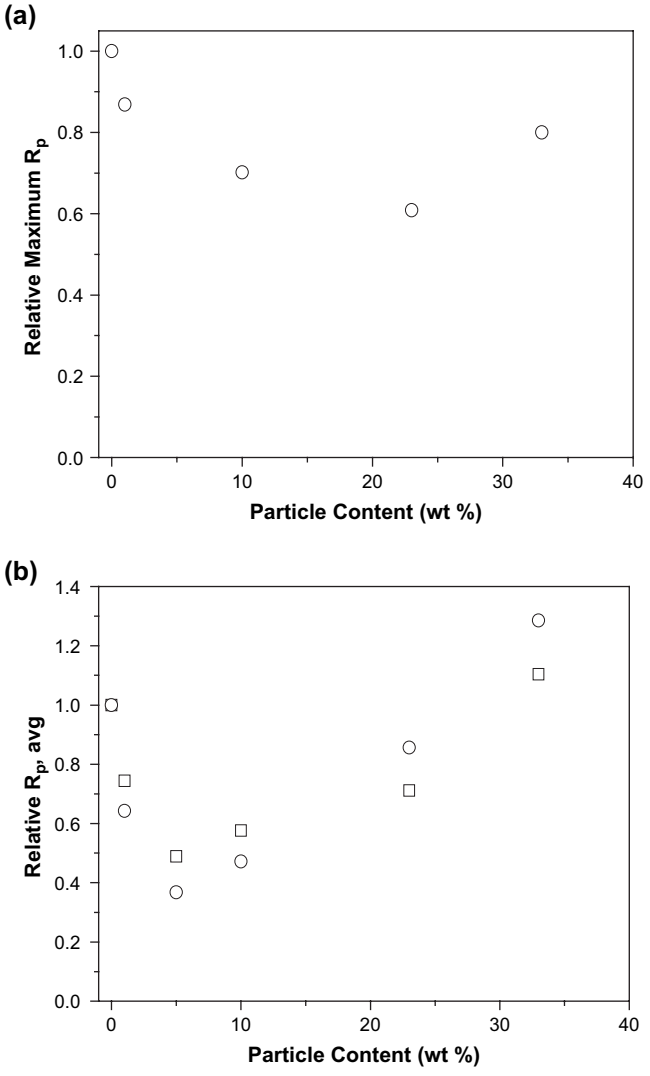

Fig. 9. (a) Relative maximum R_p and (b) relative average R_p up to 5% (○) and 50% (□) conversion as a function of particle content. Samples contain 0.5 wt% D1173 and are irradiated at 14.5 mW/cm^2 using 320–500 nm light.

4. Conclusions

The effects of surface thiol functional groups from nanoparticles on thiol–ene photopolymerization kinetics have been investigated. The viscosity of monomer/particle mixtures, the light intensity reduction, and the polymerization kinetics at the particle surface were investigated to explain the results. The unmodified nanoparticles do not exhibit any effect on the polymerization kinetics. However, small changes with unique tendencies were observed when thiol group functionalized particles were used. Thiol functional groups on the particle surface cause a stoichiometric imbalance between ene and thiol groups at the particle surface. The excess thiol concentration at the particle surface results in slow thiyl radical addition to the ene bonds due to the relatively low ene concentration and hindered thiyl radical mobility. In acrylate group functionalized particles/acrylate mixtures, the particles do not affect the polymerization kinetics, indicating that the functional group imbalance is a primary reason for decreasing polymerization rates in thiol–ene polymerizations. With high loading of thiol functionalized particles, polymerization rates were enhanced. Because of particle proximity when high concentrations of particles were added, it is expected that reaction-induced viscosity enhancement causes the incorporation of nanoparticles into the crosslinked networks, resulting in increase in viscosity and conversion rates of thiol–ene polymerizations, especially at the initial stage of polymerization. Thiol–ene nanocomposites show advantageous aspects compared to the acrylate systems. Because of reduced oxygen inhibition and the low viscosity of thiol–ene polymerization, thiol–ene nanocomposites exhibited less reduction in final conversion and no induction period.

Acknowledgements

The authors acknowledge the Fundamentals and Applications of Photopolymerizations NSF IUCRC for funding of this work.

References

[1] Keller L, Decker C, Zahouily K, Benfarhi S, Le Meins JM, Miehe-Brendle J. Polymer 2004;45:7437.
[2] Benfarhi S, Decker C, Keller L, Zahouily K. Eur Polym J 2004;40:493.
[3] Xu GC, Li AY, Zhang LD, Wu GS, Yuan XY, Xie T. J Appl Polym Sci 2003;90:837.
[4] Cho J, Ju H, Hong J. J Polym Sci Part A Poly Chem 2005;43:658.
[5] Shemper BS, Morizur J-F, Alirol M, Domenech A, Hulin V, Mathias LJ. J Appl Polym Sci 2004;93:1252.
[6] Liu G, Zhang L, Qu X, Wang B, Zhang Y. J Appl Polym Sci 2003; 90:3690.
[7] Crivello JV, Mao Z. Chem Mater 1997;9:1562.
[8] Kim WS, Houbertz R, Lee T, Bae B. J Polym Sci Part B Polym Phys 2004;42:1979.
[9] Bosch P, Del Monte F, Mateo JL, Levy L. J Polym Sci Part A Polym Chem 1996;34:3289.
[10] Nie J, Rabek JF, Linden L-A. Polym Int 1999;48:129.
[11] Fouassier J-P. Photoinitiation photopolymerization and photocuring: fundamentals and applications. Munich, Vienna, New York: Hanser Publishers; 1995.
[12] Papas P. Radiation curing, science and technology. NY: Plenum Press; 1992.
[13] Morgan CR, Magnotta F, Ketley AD. J Polym Sci Part A Polym Chem 1977;627.
[14] Jacobine AF. In: Fouassier JD, Rabek JF, editors. Radiation curing in polymer science and technology III, polymerisation mechanisms, vol. 3. London: Elsevier Applied Science; 1993. p. 219.
[15] Hoyle CE, Lee TY, Roper T. J Polym Sci Part A Polym Chem 2004;42:5301.
[16] Morgan CR, Magnotta F, Ketley AD. J Polym Sci Polym Chem Ed 1977;15:627.
[17] Gush DP, Ketley AD. Mod Paint Coatings 1978;68:58.
[18] Bor-Sen C, Khan SA. Macromolecules 1997;30:7322.
[19] Carioscia JA, Lu H, Stanbury JW, Bowman CN. Dent Mater 2005;21:1137.
[20] Cramer NB, Scott JP, Bowman CN. Macromolecules 2002;35:5361.
[21] Cramer NB, Bowman CN. J Polym Sci Part A Polym Chem 2001;39:3311.
[22] Cramer NB, Reddy SK, Cole M, Hoyle CE, Bowman CN. J Polym Sci Part A Polym Chem 2004;42:5817.
[23] Lovell LG, Berchtold KA, Elliott JE, Lu H, Bowman CN. Polym Adv Technol 2001;12:335.
[24] Van Dijk JTM. PCT Int Appl 2000;33.
[25] Lee TY, Kaung W, Jonsson ES, Lowery K, Guymon CA, Hoyle CE. J Polym Sci Part A Polym Chem 2004;42:4424.
[26] Bartholome C, Beyou E, Bourgeat-Lami E, Chaumont P, Zydowicz N. Macromolecules 2003;36:7946.
[27] Reddy SK, Cramer NB, Bowman CN. Macromolecules 2006;39: 3673.
[28] Cramer NB, Davies T, O'Brien AK, Bowman CN. Macromolecules 2003;36:4631.
[29] Cramer NB, Reddy SK, O'Brien AK, Bowman CN. Macromolecules 2003;36:7964.
[30] Roper TM, Kwee T, Lee TY, Guymon CA, Hoyle CE. Polymer 2004;45:2921.
[31] Kloosterboer JG. Adv Polym Sci 1988;84:1.